Optical alignment of the Solar Orbiter EUI flight instrument

A. Mazzoli*[a], J.-P. Halain[b], F. Auchère[c], J. Barbay[c], S. Meining[d], A. Philippon[c], G. Morinaud[c], S. Roose[a], M.-L. Hellin[a], L. Jacques[a], U. Schühle[d], C. Dumesnil[c], R. Mercier[e], E. Renotte[f], P. Rochus[a]

[a]Centre Spatial de Liège, Avenue du Pré Aily, Liege Science Park, 4031 Angleur, Belgium; [b]ESTEC – European Space Research and Technology Center, Keperlaan 1, 2201 AZ Noordwijk, The Netherlands; [c]Institut d'Astrophysique Spatiale, Bât 120-121, Université Paris-Sud, 91405 Orsay Cedex, France; [d]Max-Planck-Institut für Sonnensystemforschung, Justus-von-Liebig-Weg 3, 37077 Göttingen, Germany; [e]Laboratoire Charles Fabry, Institut d'Optique Graduate School, 2 avenue Augustin Fresnel, 91127 Palaiseau Cedex, France; [f]AMOS, Liege Science Park, 2 Rue des Chasseurs Ardennais, 4031 Angleur, Belgium.

ABSTRACT

The Extreme Ultraviolet Imager (EUI) instrument for the Solar Orbiter mission will image the solar corona in the extreme ultraviolet (17.1 nm and 30.4 nm) and in the vacuum ultraviolet (121.6 nm). It is composed of three channels, each one containing a telescope.

Two of these channels are high resolution imagers (HRI) at respectively 17.1 nm (HRI-EUV) and 121.6 nm (HRI-Lyα), each one composed of two off-axis aspherical mirrors. The third channel is a full sun imager (FSI) composed of one single off-axis aspherical mirror and working at 17.1 nm and 30.4 nm alternatively. This paper presents the optical alignment of each telescope.

The alignment process involved a set of Optical Ground Support Equipment (OGSE) such as theodolites, laser tracker, visible-light interferometer as well as a 3D Coordinates Measuring Machine (CMM).

The mirrors orientation have been measured with respect to reference alignment cubes using theodolites. Their positions with respect to reference pins on the instrument optical bench have been measured using the 3D CMM. The mirrors orientations and positions have been adjusted by shimming of the mirrors mount during the alignment process.

After this mechanical alignment, the quality of the wavefront has been checked by interferometric measurements, in an iterative process with the orientation and position adjustment to achieve the required image quality.

Keywords: Extreme Ultraviolet, Solar Orbiter, Flight Model, Alignment

1. INTRODUCTION

On-board the Solar Orbiter mission, the Extreme Ultraviolet Imager (EUI)[1,2,3,4] is one of the six remote-sensing instruments. The EUI instrument is dedicated to observations of the solar corona at the extreme ultraviolet (EUV) wavelengths of 17.4 and 30.4 nm and the vacuum ultraviolet (VUV) wavelength of 121.6 nm. The development of the EUI instrument has been successfully completed, among other tasks, with the optical alignment of its three channels. The present paper describes the processes involved in this alignment.

*amazzoli@uliege.be

2. OPTICAL ALIGNMENT

The EUI instrument is composed of three channels, each one containing a telescope. Two of these channels are high resolution imagers (HRI) working at respectively 17.1 nm (HRI-EUV) and 121.6 nm (HRI-Lyα), each one composed of two off-axis aspherical mirrors. The third channel is a full sun imager (FSI) composed of one single off-axis aspherical mirror and working at 17.1 nm and 30.4 nm alternatively. The fields of view (FOV) of the three channels are respectively 0.28 arcdeg for the HRI channels and 5.2 arcdeg for the FSI channel. The optical design of these three channels has already been described in previous papers[5,6,7].

The optical alignment of the three telescopes involved a set of Optical Ground Support Equipment (OGSE) such as theodolites, laser tracker, visible-light interferometer and a 3D Coordinates Measuring Machine (CMM). The alignment activities included position and orientation adjustment of the mirrors as well as interferometric measurements of each channel's wavefront error (WFE). An iterative process between these activities was necessary to obtain the expected imaging quality for each telescope.

2.1 EUI Optical Bench System

The three channels are mounted on a common Optical Bench System (OBS) unit. The OBS includes a Unit Alignment Reference Frame (UARF) materialized by an alignment cube on the instrument front side and a mechanical Unit Reference Frame (URF) centered on a fixation hole of one OBS structure foot and materialized by two pins located on the main bench of the OBS structure. Figure1 shows the OBS reference frames with the three channels Line of Sight (LoS) and the Instrument Line of Sight (ILS) which is the average of the three channels LoS. An additional alignment cube, co-aligned with the UARF, was attached to the OBS back side in order to have an easier access to the UARF from both front and back sides of the OBS. The horizontal (Hz) and vertical (V) tilts as used for the alignment are also shown on Figure 1 (with yaw/pitch correspondence). The mirrors orientation were measured with respect to the UARF using theodolites, while their position were measured with respect to the URF using the 3D CMM.

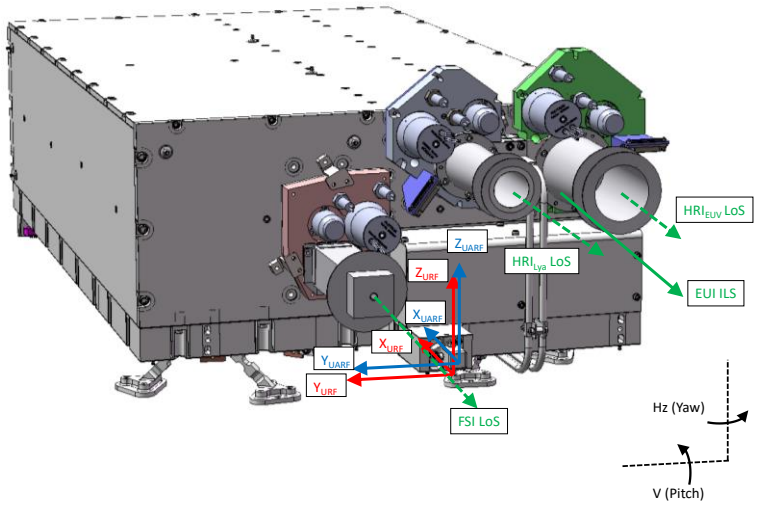

Figure 1. EUI OBS unit reference frames

2.2 HRI-EUV channel

2.2.1. Mirrors positioning

For both mirrors of the HRI-EUV channel, two uncoated reference surfaces, whose orientation with respect to the mirror optical axis was measured during manufacturing, are available for the mirrors orientation measurements with theodolites.

One reference surface is on the back of the mirrors (on the opposite side of the coated surface) and is used to align the mirrors optical axis with respect to the UARF. The other reference surface is on the lateral side of the mirrors and is used to measure the roll of the mirrors.

The first mirror (M1) of the channel has been positioned and oriented to align its optical axis with the mechanical axis of the OBS (which corresponds to the X axis of the URF). As there was no access to the URF with theodolites, M1 optical axis was actually aligned on the UARF X axis, the relative orientation of the UARF with respect to the URF being known from OBS manufacturer measurements. The adjustments on M1 orientation were performed with shims of different thicknesses located at the three fixation points to the OBS back panel (Figure 2).

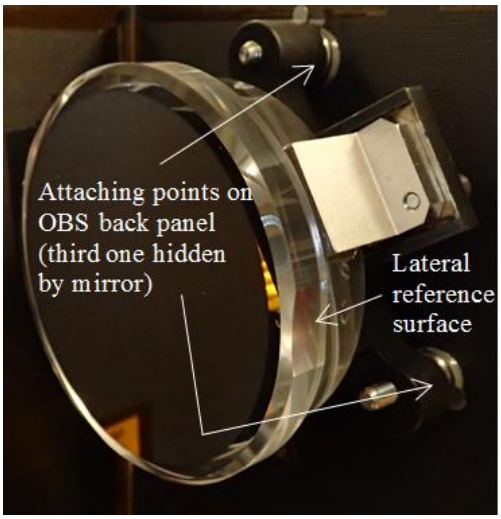

Figure 2. HRI-EUV M1 mirror with its mounting interface

The second mirror (M2) of the HRI-EUV channel has been mounted on the bottom panel of the OBS and aligned with respect to the M1 optical axis according to its nominal orientation and position as per design. As for M1, shims have been used inside the mounting to adjust M2 orientation. Figure 3 shows a picture of M2.

Figure 3. HRI-EUV M2 mirror with its mounting structure

The final M1 and M2 optical axes orientation and roll errors are presented in the tables below. The side reference surface of M1 has been adjusted to be close to vertical (angle = 0°) and the side reference surface of M2 has been adjusted to compensate the difference between the two mirrors off-axis directions.

Table 1. HRI-EUV mirrors optical axes final orientations

Element	Orientation	Value
M1 optical axis w.r.t. front cube	Hz	19′′
	V	1′ 04′′
M2 optical axis w.r.t. M1 optical axis	Hz	1′ 40′′
	V	2′ 17″

Table 2. HRI-EUV mirrors final roll errors

Element	Orientation	Value
M1 side reference surface	V	0.088°
M2 side reference surface	V	0.555°

The position of the mirrors front face physical center has been determined from 3D measurements of the reference surfaces of the mirrors (the back and lateral reference surfaces) and the external cylinder. The URF is first measured from the front foot reference hole and the two reference pins of the main bench panel, defining the bench mechanical axis. The horizontal and vertical positions of the mirrors center in the URF and the corresponding deviation with respect to the nominal mirrors distances have then been deduced. The distance measured between the two mirrors centers is 655.881 mm corresponding to a difference of 200 µm with respect to the nominal distance. An accuracy of 10 µm on the distance between the two mirrors is however needed to have an acceptable focus term on the telescope WFE. Such accuracy is not achievable only by 3D measurements. To cope with this an interferometric measurement has been used to finalize the alignment with iterations on mirrors position shimming.

2.2.2. Interferometric measurements

The first foreseen interferometric alignment method (so-called “front-side method”) used a transmission flat as reference wavefront on the interferometer to illuminate the instrument through its entrance aperture with a collimated beam and a small aluminum ball at the focal plane position. The obtained interferograms showed unexpected parasitic patterns and aberrations which made these measurements not usable. It was thus decided to reverse the setup (so-called “back-side method”) and illuminate the instrument with a spherical beam through its focal plane (Figure 4 left). A λ/20 flat mirror was then used at the instrument entrance to close the interferometric cavity. A small fold was placed after the channel focal plane to bend the beam and to give room for the interferometer installation.

The impossibility to obtain measurable interferograms with the front-side method is due to the large F-number of the telescope equal to almost 90. The beam divergence θ after reflection on the two mirrors is thus equal to 5.5 mrad. As the interferometer laser beam can be considered as gaussian, the associated beam waist w_0 can be calculated from the formula[8,9] $\theta = \frac{\lambda}{\pi \cdot w_0}$ which gives w_0 = 36 µm. The beam Rayleigh range z_R can be obtained from the beam waist following $z_R = \frac{\pi \cdot w_0^2}{\lambda}$ and is equal to 6.5 mm which is of the order of magnitude of the aluminum ball radius of curvature (6.35 mm for a 0.5” diameter ball). The radius of curvature of the wavefront at the surface of the ball (i.e. for z = 6.35 mm) is calculated with formula (1) which applies to Hermite-Gaussian modes. The obtained radius is equal to 13 mm which is larger than the ball radius of curvature giving errors on the phase of the reflected wavefront.

$$R(z) = z\left[1+\left(\frac{z_R}{z}\right)^2\right] \quad (1)$$

With the reversed setup, a first WFE has been measured to determine the wavefront residual focus term, allowing to calculate the needed compensating movement on M2 focus. The corresponding shims were implemented without

changing M2 orientation and the final WFE of the telescope was then measured (see Figure 4 right, the average result of 10 WFE). The Zernike coefficients of this averaged WFE are all below 0.01 waves, the Peak-Valley (PV) and Root Mean Square (RMS) amplitudes being within specifications with 0.057 waves (⇔ 36 nm) and 0.009 waves (⇔ 5.7 nm) respectively. For the final measurement, the flat orientation has been corrected by 16 arcsec in horizontal and 11 arcsec in vertical to cancel the tilt in the WFE. As a result, the measured WFE does not exactly correspond to the central part of the Field of View (FOV) of the instrument but it is very close to it (16 arcsec and 11 arcsec, i.e. less than 1% from the FOV center).

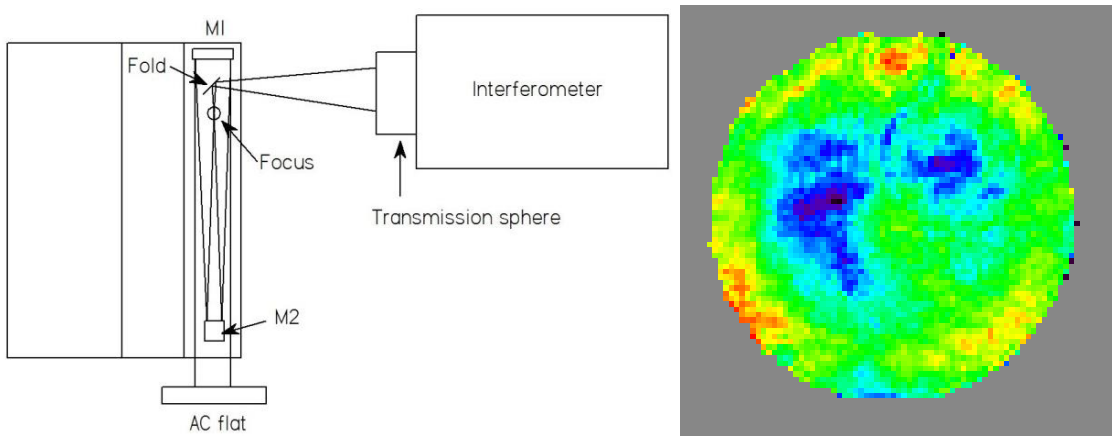

Figure 4. (Left) HRI-EUV interferometric back-side method, (Right) Average of HRI-EUV final alignment WFE

The residual focus error of 0.009 waves measured with the interferometer corresponds to a defocus of 0.7 mm in the focal plane. The detector should have been moved towards M2 for compensation of this defocus and an additional 0.12 mm should also have been added to be at the best focus for the entire FOV and not only the central part of it. A maximum correction of 0.5 mm was however possible to implement on the detector support structure, leaving 0.32 mm between the detector real position and the best focus position. From ray tracing simulations, the corresponding residual focus error due to this 0.32 mm corresponds to an increase of less than 2 µm on the image spot sizes (the RMS diameter being 7 µm without residual focus), which was considered as fully acceptable for the channel performance.

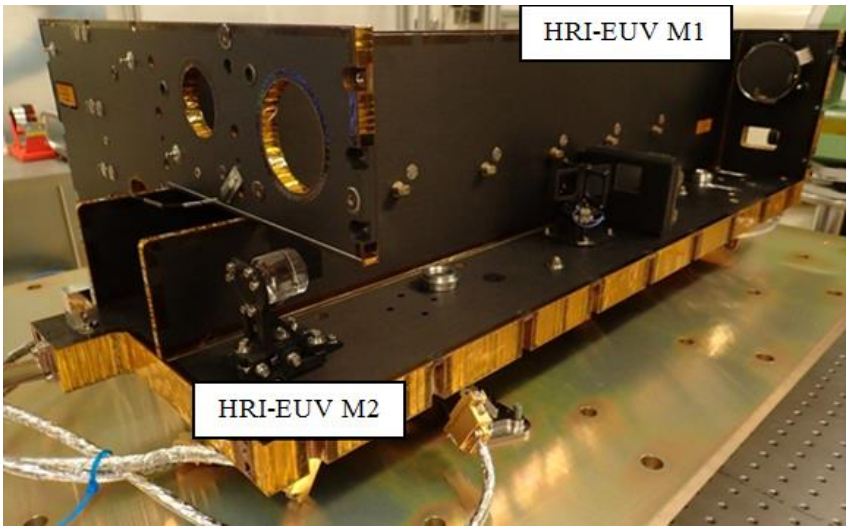

Figure 5. HRI-EUV mirrors on EUI OBS

2.3 HRI-Lyα channel

The HRI-Lyα channel is a Gregory design with an effective focal length of 5804 mm. Prior to the mirrors final installation on the flight optical bench, the interferometric alignment of the two mirrors has been performed on a dummy optical bench simulating the OBS. The mirrors have then been transferred to the flight bench by geometrical verification of the alignment. As for the HRI-EUV channel, the mirrors orientation with respect to the reference cube (UARF) have been measured with theodolites and their position with respect to theoretical positions from the optical model have been checked with the CMM. Figure 2 shows the mirrors mounted to the OBS back side (M1) and bottom panel (M2) including the camera with a high voltage unit.

Interferometric verification on the flight bench proved unfeasible due to lack of room and accessibility inside the central part of the OBS housing. The verification of focus position was deemed unnecessary due to the large tolerance of this channel's optical design.

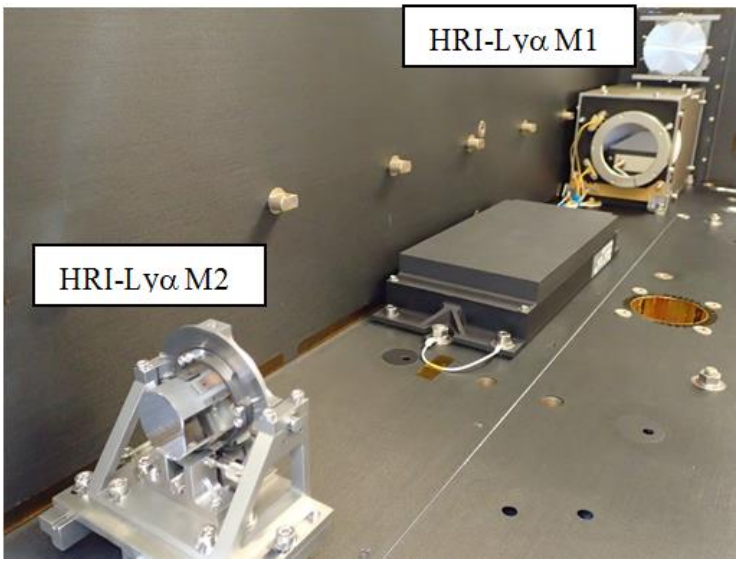

Figure 6. HRI-Lyα mirrors and camera mounted on the EUI OBS

2.4 FSI channel

For the FSI channel, the mirror was aligned with respect to the mechanical axis using the alignment cubes and theodolites. A dummy camera composed of an array of micro lenses was used for the interferometric measurements on axis and for different positions in the FOV. The alignment has been performed using the central FOV and verified for three other FOVs. At the end of the process, the measured distance between the focal plane and the mirror was only 20 µm from the theoretical value, the FSI channel being so aligned within specified tolerances. 3D measurements of the channel were furthermore performed to assess the correct positioning of the mirror and the camera. The FSI channel filter wheel was also aligned within the tolerance budget of ± 0.2° with respect to the optical axis. The obtained residual misalignments between the optical axis and the mechanical axis are given in the Table 3 below.

Table 3. FSI mirror residual misalignment between optical and mechanical axis

Angle	Value
Δθ Y (horizontal)	+33″
Δθ X (vertical)	-1′02″
Δθ Z (roll)	+1″

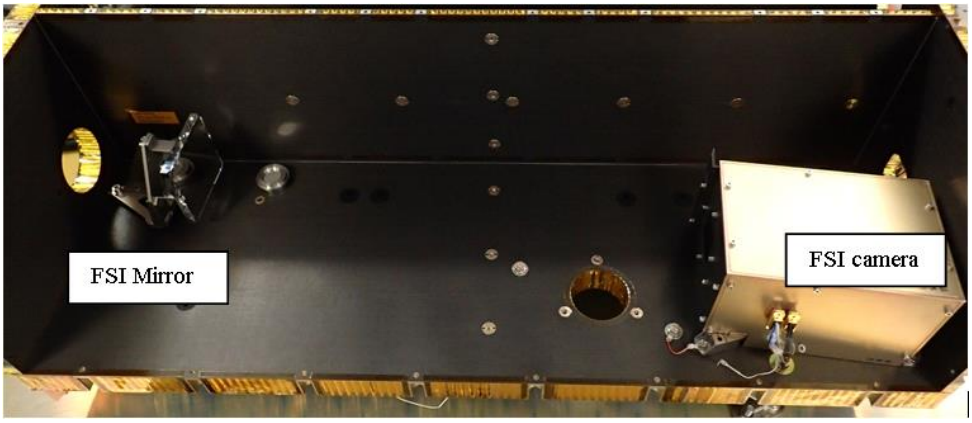

Figure 7. FSI mirror and camera on EUI OBS

2.5 Channels co-alignment

In addition to their respective optical alignment the three EUI channels have also to be co-aligned as much as possible with respect to the UARF. The Instrument Line of Sight (ILS) was then considered as the average of the two HRI channels LoS (the channels with smaller FOV). The ILS offset vs. UARF and vs. URF are summarised in Table 4, where the offset accuracy is < 20 arcsec.

Table 4. EUI ILS w.r.t. UARF and URF

	ILS vs. UARF	UARF vs. URF	ILS vs. URF	
Hz	-1 arcsec	+70 arcsec	+69 arcsec	+ clockwise (around +ZEUI) - YawEUI
V	+7 arcsec	-60 arcsec	-53 arcsec	+ clockwise (around +YEUI) - PitchEUI

3. CONCLUSIONS

The alignment of the EUI instrument three channels has been presented. An iterative mechanical alignment of the mirrors with the help of theodolites and a 3D CMM combined with interferometric verifications permitted to achieve the expected performances for each channel as well as an acceptable co-alignment of the 3 channels.

ACKNOWLEDGEMENTS

The EUI instrument was developed in a collaboration including the Centre Spatial de Liège (Belgium), the Institut d'Astrophysique Spatiale and the Institut d'Optique (France), the UCL Mullard Space Science Laboratory (UK), the Max Planck Institute for Solar System Research (Germany), the Physikalisch-Meteorologisches Observatorium Davos (Switzerland), and the Royal Observatory of Belgium (Belgium).

The Belgian institutes are funded by Belgian Federal Science Policy Office (BELSPO); the French institutes by Centre National d'Etudes Spatiales (CNES); the UK institute by the UK Space Agency (UKSA); the German institute by Deutsche Zentrum für Luft- und Raumfahrt e.V. (DLR), and the Swiss institute by the Swiss Space Office (SSO).

REFERENCES

[1] Rochus P., Halain J.P., Renotte E., Berghmans D., Zhukov A., Hochedez J.F., Appourchaux T., Auchère F., Harra L.K, Schühle U., Mercier R.., "The Extreme Ultraviolet Imager (EUI) on-board the Solar Orbiter Mission," 60th International Astronautical Congress, (2009).

[2] Hochedez J.-F., Appourchaux T., Defise J.-M., Harra L. K., Schuehle U., Auchère F., Curdt W., Hancock B., Kretzschmar M., Lawrence G., Marsch E., Parenti S., Podladchikova E., Rochus P., Rodriguez L., Rouesnel F., Solanki S., Teriaca L., Van Driel L., Vial J.-C., Winter B., Zhukov A., "EUI, The Ultraviolet Imaging Telescopes of Solar Orbiter," The Second Solar Orbiter Workshop, (2006).

[3] Halain J.-P., Rochus P., Appourchaux T., Berghmans D., Harra L., Schühle U., Auchère F., Zhukov A., Renotte E., Defise J.-M., Rossi L., Fleury-Frenette K., Jacques L., Hochedez J.-F., Ben Moussa A., "The technical challenges of the Solar-Orbiter EUI instrument," Proc. SPIE 7732, 26 (2010).

[4] Schühle U., Halain J., Meining S., Teriaca L., "The Lyman-alpha telescope of the extreme ultraviolet imager on Solar Orbiter," Proc. SPIE Solar Physics and Space Weather Instrumentation IV, 8148, (2011).

[5] Halain J.-P., Rochus P., Renotte E., Auchère F., Berghmans D., Harra L., Schühle U., Schmutz W., Zhukov A., Aznar Cuadrado R., Delmotte F., Dumesnil C., Gyo M., Kennedy T., Mercier R., Verbeeck C., Thome M., Heerlein K., Hermans A., Jacques L., Mazzoli A., Meining S., Rossi L., Tandy J., Smith P., Winter B., "The Extreme UV Imager of Solar Orbiter – From detailed design to Flight Model," Proc SPIE, 9144, (2014).

[6] Halain J.-P., Rochus P., Renotte E., Hermans A., Jacques L., Auchère F., Berghmans D., Harra L., Schühle U., Schmutz W., Zhukov A., Aznar Cuadrado R., Delmotte F., Dumesnil C., Gyo M, Kennedy T., Smith P., Tandy J., Mercier R., Verbeeck C., "The Extreme UV Imager telescope on-board the Solar Orbiter mission – Overview of phase C and D," Proc SPIE, 9604, (2015).

[7] Halain J.-P., Renotte E., Auchère F., Berghmans D., Felmotte F., Harra L., Schmutz W., Schühle U., Aznar Cuadrado R., Dumesnil C., Gyo M., Kennedy T., Verbeeck C., Barbay J., Giordanengo B., Gissot S., Gottwald A., Heerlein K., Hellin M.-L., Hermans A., Hervier V., JacquesL., Laubis C., Mazzoli A., Meining S., Mercier R., Philippon, A., Roose S., Rossi L., Scholze F., Smith P., Teriaca L., Zhang X., Rochus P., "The EUI flight instrument of Solar Orbiter – From Optical Alignment to End-to-End Calibration, " Proc SPIE, 10699, (2018).

[8] Kogelnik H., Li T., "Laser beams and resonators," Applied optics IP, vol. 5, Issue 10, p.1550, 10/1966.

[9] Svelto O., [Principles of Lasers], 5th edn., Springer, (2010).